Stability of Organic Permeable Base Transistors

Kashi N. Subedi,[1, a)] Akram Al-Shadeedi,[1, b)] and Björn Lüssem[1, c)]
Department of Physics, Kent State University, Kent, OH 44240, USA

(Dated: June 11, 2020)

Organic Permeable Base Transistors (OPBTs) reach a very high transit frequency and large on-state currents. However, for a later commercial application of this technology, a high operational stability is essential as well. Here, the stability of OPBTs during continuous cycling and during base bias stress is discussed. It is observed that the threshold voltage of these transistors shifts towards more positive base voltages if stressed by applying a constant potential to the base electrode for prolonged times. With the help of a 2D device simulation, it is proposed that the observed instabilities are due to charges that are trapped on top of an oxide layer formed around the base electrode. These charges are thermally released after removing the stress and the device reaches its initial performance after around 24-48 hours.

Keywords: Organic Transistors, Organic Permeable Base Transistor, Stability, Base-Bias Stress

A wide range of applications are enabled by the inherent flexibility of organic transistors, and bendable or even foldable displays have moved into the focus of research[1]. Organic Permeable Base Transistors (OPBTs) are a relatively young but highly promising type of organic transistors. OPBTs have a unique vertical structure, shown in Figure 1. They consist of three electrodes (emitter, base and collector), which are separated by a layer of an organic semiconductor. The base electrode, often consisting of aluminum, is very thin and not fully closed, i.e. small openings remain in the electrode. Furthermore, the base electrode is exposed to ambient air after processing to grow a thin oxide layer on its surface.

The vertical structure of OPBTs allows for a switching mechanism distinctively different to conventional field-effect transistors. Current injected at the upper emitter electrode is transmitted through the small holes in the base electrode and finally collected by the bottom electrode. This vertical current can be controlled by the base potential, i.e. the current can be switched "OFF" or "ON" if the potential difference between the injecting contact and the base electrode is varied.

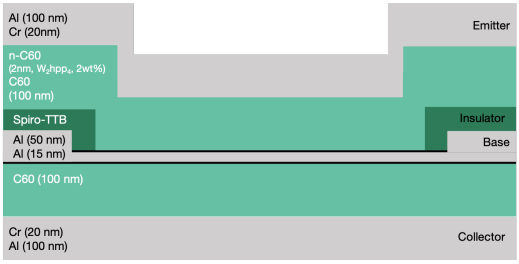

Figure 1: Structure of the Organic Permeable Base Transistor studied here.

The OPBT structure allows to tune the device thickness with nanometer precision, which leads to a high performance[2–5]. A high switching ratio (10^8), large on-state current densities (75 A/cm^2) at low voltages (2 V), and a large transient frequency up to 40 MHz have been reported[6]. Numerical modeling has shown that OPBTs have the potential to reach even switching frequencies in the range of 100 MHz[7]. Furthermore, current amplification ratios as large as 10^5 were reported.

This excellent performance, in particular the large current amplification reached recently, makes OPBTs a potential alternative to other thin film transistor technologies used as driving transistor in active matrix OLED displays[8]. However, this application poses strict requirements on the stability of the device characteristics, in particular the threshold voltage, under electrical stress. The driving transistor in a backplane of an OLED display has to continuously drive a pre-set current through the OLED. Any shift in the threshold voltage during operation will therefore result in an unwanted dimming of the pixel. Furthermore, a different driving history of different pixels will lead to a brightness variation across the display, which is easily noticeable.

In this paper, the operational stability of OPBTs is studied. In particular, the shift in the transfer characteristic under continuous cycling and under constant base bias stress is discussed. It is shown that the transfer characteristic of these devices shifts constantly while cycling, and, akin to gate bias stress of organic field-effect transistors, under a constant bias applied to the base electrode. With the help of a two-dimensional device model, these effects are discussed in terms of trapping of charges at the base electrode.

All devices were prepared by thermal evaporation under high vacuum conditions with pressure between 10^{-7}-10^{-8} Torr, similar to the devices discussed in reference[9]. The devices were structured by laser cut metallic shadow masks to define an active area of 0.04 mm^2, 0.025 mm^2 and 0.01 mm^2. Optical images of the structure of these devices can be found in the supplemental material of

[a)] current address: Department of Physics and Astronomy, Ohio University, Athens, OH 45701, USA; Electronic mail: ks173214@ohio.edu
[b)] current address: Department of Physics, University of Baghdad, Al-Jadriya, Baghdad 10071, Iraq
[c)] Electronic mail: blussem@kent.edu

reference[9]. Glass substrates were cleaned by sonication in acetone, methanol and iso-propanol, and the cleaned substrates were dried by blowing pure air.

The substrates were loaded in a vacuum chamber followed by the deposition of the different layers shown in Fig. 1. First, 100 nm of Al was deposited at a rate of 0.5 Å/s, followed by the deposition of 20 nm of Cr at a rate of 0.1 Å/s to form a bottom contact used as collector electrode. 100 nm of an intrinsic, i.e. undoped, layer of the organic semiconductor C_{60} (i-C_{60}) was deposited on the top of Cr at a rate of 0.5 Å/s. A thin layer of Al (15 nm) was deposited on the top of the i-C_{60} to form a base electrode. An extra 50 nm thick layer of Al is deposited outside the active area of the device to improve the contact layer of a base as shown in Fig. 1.

After deposition of the base electrode, the overall Al/Cr/i-C_{60}/Al stack (also termed the bottom diode) was exposed to pure air for 30 to 90 minutes placed close to a reservoir of distilled water to form a thin insulating layer of Al_2O_3($\approx$ 2-3 nm) on the base Al. The variation in exposure time has a small influence on the ON/OFF ratio of the transistor, as discussed in reference[9]. Afterwards, the devices were annealed at 60°C for four hours before they were transferred back to the deposition chamber. To define the active area of the device, a bank structure of 200 nm of Spiro-TTB (2,2′,7,7′-Tetra(N,N -di-p -tolyl)amino-9,9-spirobifluoreneSpiro-TTB, Lumtec Corp.) was deposited at a rate of 0.5 Å/s. Overall, controlling the device area by this additional Spiro-TTB layer was shown to increase the performance of OPBTs[9]. After the deposition of the Spiro-TTB layer, 100 nm of i-C_{60} was deposited. To improve the charge injection in the devices, 20 nm of n-doped C_{60} (n-dopant W_2hpp_4, 2wt.%) was deposited on top of i-C_{60}. This deposition step was followed by deposition of 20 nm Cr and 100 nm Al to form the top emitter contact and to complete the OPBT structure.

Devices were then annealed at 150°C in ambient air, which was shown to improve the performance of OPBTs[10]. Finally, the devices were tested with a semiconductor parameter analyzer (Keithley 4200).

The stability of OPBTs is tested under two distinct modes of operation. In the first mode, the device is cycled for an extended time, i.e. the transfer characteristics is measured consecutively for several minutes. In a second mode, the stability is tested when a constant voltage is applied to the base electrode, which is closer to a potential application of OPBTs as driving transistors in display backplanes.

Fig. 2a shows the transfer characteristic of an OPBT cycled for 27 minutes. The collector-emitter voltage V_{CE} is kept at 2 V. A small shift in the transfer characteristics is clearly visible. Overall, the transfer characteristic of the device shifts towards more positive base-emitter voltages V_{BE} for the first 10 minutes, after which the shift saturates. The shift in the transfer characteristic is correlated to a shift in the threshold voltage, which is plotted is shown in Fig. 2b. As seen in Fig. 2b, the

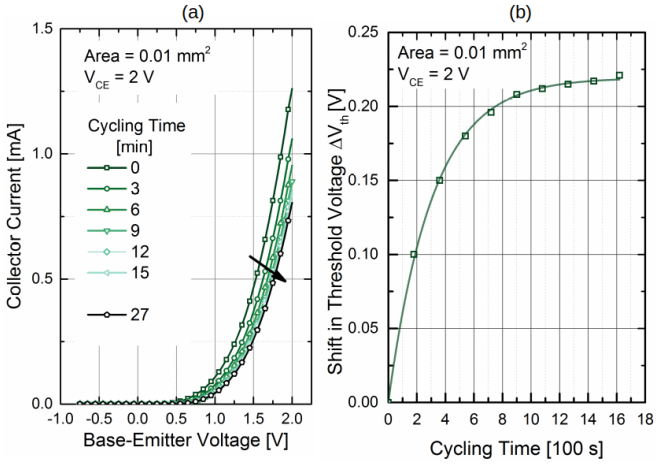

Figure 2: **Stability of OPBTs under continuous cycling.** a) A small shift in the transfer characteristics is observed during cycling, which saturates quickly. b) Shift in threshold voltage with time. Experimental results are plotted by symbols and the continuous line is a fit using Eq. (1).

voltage shift depends exponentially on the cycling time. It can be fitted by a stretched exponential relation given by

$$\Delta V_{th} = (\Delta V_{th})_\infty [1 - e^{-(\frac{t}{\tau})^\beta}] \quad (1)$$

where $(\Delta V_{th})_\infty$ is the equilibrium shift in threshold voltage (i.e. for $t \to \infty$), τ is the relaxation time and β is the stretching parameter. We find a time constant of τ = 245 s and a stretching parameter β of 0.9, i.e. relatively close to 1. Overall, the shift in the threshold voltage is small (around ΔV_{th} = 0.2 V), and saturates quickly.

To study the effect of constant stress on the transistor performance, the base of the OPBT is biased at V_{BE} = 2 V, while the collector is biased at three different voltages (V_{CE} = 1 V, 1.5 V, and 2 V). After stressing the device, the transfer characteristics is measured and the shift in threshold voltage is calculated. Furthermore, the shift in the collector current at the particular base and collector potential is monitored.

The results are shown in Fig 3a. Overall, the shift in the transfer characteristics is stronger compared to the cycling experiment shown in Fig. 2b. The threshold voltage shifts by approx. ΔV_{th} = 0.7 V for a stress time of 1200 s, which does not depend on the particular collector bias V_{CE} (cf. Figure 3b). Interestingly, the shift in threshold voltage does not fully saturate, in contrast to the shift in threshold voltage observed in the cycling experiment.

In contrast to the shift in threshold voltage, the decrease in collector current strongly depends on the applied collector bias V_{CE} and increases from approx. ΔI_C = 1.5 mA at V_{CE} = 1 V to ΔI_C = 3 mA at V_{CE} = 2 V (cf. Figure 3c).

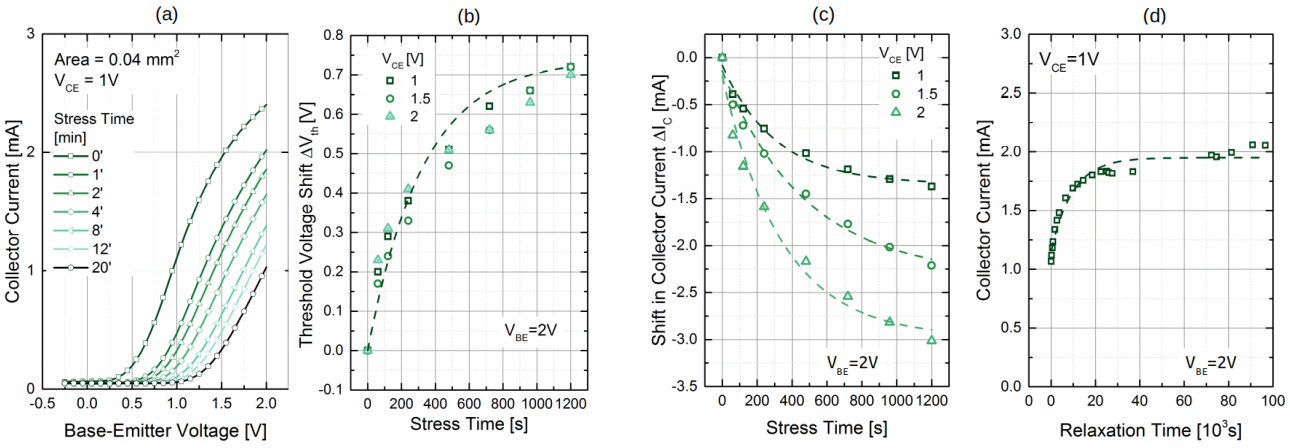

Figure 3: **Base-Bias Stress.** a) The transfer characteristics shifts for increasing stress time. b) Threshold voltage shift ΔV_{th} calculated from the transfer characteristics for different V_{CE}. c) Shift in collector current I_C with stressing time for a base-bias voltage $V_{BE} = 2$ V. d) Collector current after the release of the stress as a function of time.

This qualitative difference between the shift in the threshold voltage and in collector current can be understood by the non-ideal output characteristic shown in Fig. S1 in the supplementary material. The different collector potentials used during stressing the device correspond to different operation regimes, i.e. the devices are operated in the linear region at $V_{CE} = 1$ V and in a weak saturation regime at $V_{CE} = 1.5$ V and 2 V. Consequently, the transconductance,

$$g_m = \frac{dI_C}{d(V_{BE})_{eff}} = \frac{dI_C}{d(V_{BE} - V_{th})}$$

is different for the different collector potentials, leading to a different change in collector currents even though the shift in the effective base-emitter voltage $(V_{BE})_{eff} = V_{BE} - V_{th}$ is identical for all collector potentials.

The base bias stress effect is partially reversible, shown in Fig. 3d. After removing the base bias, the collector current is monitored for several hours. It is found that I_C almost returns to its initial value after 27 hours.

The base bias stress shown in Fig. 3 resembles gate bias stress effects in conventional Organic Field-Effect Transistors (OFETs)[11,12]. Often, it is argued that the shift in threshold voltage of OFETs is due to trapping of charges in different operation regimes. The trapping of charges in OFETs may occur i) between the interface of dielectric material and the semiconductor material[13], ii) within the bulk material[14], iii) around the defects of the semiconductor material[15], or the observed shift might be due to iv) formation of bipolarons in the semiconductor[16,17]. Increasing the stress time increases the number of trapped charges thus resulting in a more pronounced threshold voltage shift.

A numerical 2D simulation is used in order to study the origin of the base bias stress observed here. The numerical model, discussed in detail in references[9,18], is sketched in Fig. 4a. A cylindrical symmetry with a single opening/hole in the base electrode at $r = 0$ nm is assumed. Following the results of Yutani et al.[19] and Kaschura et al.[20], the base electrode (thickness of d_{base} = 12 nm) is covered with a thin Al_2O_3 layer (d_{ox} = 2 nm), which suppresses injection at the base. The C_{60} layer (total thickness between emitter and collector $d_{C_{60}}$ = 200 nm) is assumed to show an electron mobility of μ_n = 0.1 $cm^2V^{-1}s^{-1}$ and a permittivity of $\epsilon_r = 3$.

Following the results of Kaschura et al.[20], OPBTs function very much like a vertical OFET instead of an organic BJT. A horizontal channel is formed that transports charge towards the pore in the base electrode at $r = 0$, qualitatively sketched in Fig. 4a. This effect, similar to the gating effect seen in OFETs, leads to the current distribution shown in Fig. S2 in the supplementary material(plotted for $V_{BE} = 1.2$ V, $V_{CE} = 2$ V), where most of the current is concentrated at the oxide/C_{60} interface.

However, the oxide covering the base electrode is grown by exposing the base to ambient air. Usually hydroxyl (-OH) groups are formed that trap electrons[21]. To include this effect in the model, a thin layer (2 nm thick) of traps is included at the interface between the Al_2O_3 insulator on top of the base electrode and the C_{60} layer. Different trap concentrations ranging from $(2 - 20) \times 10^{19}$ cm^{-3} are assumed to model the consecutive shift in the transfer characteristics with increasing stress time. These values correspond to an interfacial trap density of $(4-40)\times10^{12}$ cm^{-2}.

The results of the simulation are shown in Fig. 4b. Indeed, the transfer characteristics of the transistor shifts continuously toward higher threshold voltages for a higher concentration of traps. This shift results from a decrease in the density of free (i.e. not trapped) charge carriers inside the channel, which leads to a shift in the threshold voltage by $\Delta V_{th} = \frac{e n_{trap} d}{C}$, where e is an elementary charge, n_{trap} is the density of trapped charges, d represents thickness of the layer of traps, $C = \frac{\epsilon_0 \epsilon_r}{d_{ox}}$ rep-

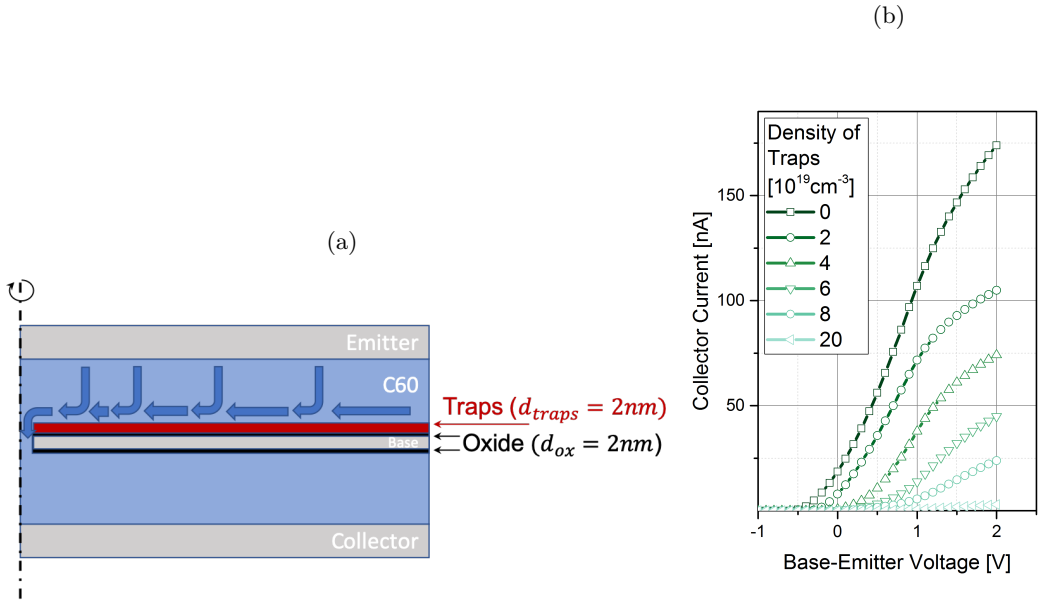

Figure 4: **Modeling base-bias stress in OPBTs.** a) Device model used to study base-bias stress in OPBTs. c) Adding trap states to this channel region leads to an increasing shift in the transfer characteristic.

resents specific capacitance of the oxide layer on top of the base electrode).

This mechanism can explain the trends observed in Fig. 2 and Fig. 3. Cycling the transistors (Fig. 2) allows to partially free electrons trapped at the Al_2O_3 surface during the negative part of the cycle, which in accordance to the experiment is expected to result in a weaker shift in threshold voltage as for a constant positive bias stress.

Furthermore, the Al_2O_3/C_{60} responsible for trapping of electrons is shielded from the collector potential, which explains that the shift in threshold voltage does not depend on the emitter-collector voltage V_{CE} as observed in Fig. 3b. Finally, the trapped electrons will be thermally released after releasing electrical stress, and the original performance is recovered, which was indeed observed in Fig. 3d.

A high operational stability is essential for the success of vertical organic permeable-base transistors. OPBTs have to show a small drift in the threshold voltage during continuous stress, in particular if they are used as driving transistor in active matrix displays.

As shown here, OPBTs are subject to similar limitations as standard organic field-effect transistors, i.e. they are susceptible to base-bias stress. Overall, the threshold voltage of OPBTs shifts by approx. 0.7 V during the first 20 minutes of stressing, which corresponds to a decrease in their on-state current by 1-3 mA.

The origin of the shift in threshold voltage due to an extended bias applied to the base is discussed with the help of a numerical device model. It is shown that the observed trends can be explained by increasing trapping at the oxide/semiconductor interface on top of the base electrode.

Understanding the mechanism of base bias stress can be used to improve the stability of OPBTs. Most importantly, the trap states at the oxide surface have to be passivated. To passivate these traps states, a conformal and insulating layer has to be found that is not blocking holes in the base electrode. Self-assembled monolayers, such as phosphonic acid base monolayers used for OFETs[22], are therefore promising candidates to optimize the stability of OPBTs.

See the supplementary materials for a more detailed experimental description, a representative output characteristic of the OPBTs discussed here, and more simulation results.

Funding from the National Science Foundation (grant no. 1639073) and from the Bi-national Science Foundation (grant no. 2014396) is greatly acknowledged. Characterization of samples was partially done at the Characterization Facility of the Liquid Crystal Institute, Kent State University. AA was supported by The Higher Committee For Education Development in Iraq.

REFERENCES

[1]S. Steudel, K. Myny, S. Schols, P. Vicca, S. Smout, A. Tripathi, B. van der Putten, J.-L. van der Steen, M. van Neer, F. Schtze, O. R. Hild, E. van Veenendaal, P. van Lieshout, M. van Mil, J. Genoe, G. Gelinck, and P. Heremans, "Design and realization of a flexible qqvga amoled display with organic tfts," Organic Electronics **13**, 1729 – 1735 (2012).

[2]K. Zhao, J. Deng, X. Wu, X. Cheng, J. Wei, and S. Yin, "Fabrication and characteristics of permeable-base organic transistors based on co-evaporated pentacene:al base," Organic Electronics **12**, 1003 – 1009 (2011).

[3]F. Kaschura, A. Fischer, D. Kasemann, K. Leo, and B. Lüssem, "Controlling morphology: A vertical organic transistor with a self-structured permeable base using the bottom electrode as seed layer," Applied Physics Letters **107**, 033301 (2015).
[4]B. Lüssem, A. Günther, A. Fischer, D. Kasemann, and K. Leo, "Vertical organic transistors," Journal of Physics: Condensed Matter **27**, 443003 (2015).
[5]K. Agrawal, O. Rana, N. Singh, R. Srivastava, and S. S. Rajput, "Low voltage organic permeable base n-type transistor," Applied Physics Letters **109**, 163301 (2016).
[6]B. Kheradmand-Boroujeni, M. P. Klinger, A. Fischer, H. Kleemann, K. Leo, and F. Ellinger, "A pulse-biasing small-signal measurement technique enabling 40 mhz operation of vertical organic transistors," Scientific Reports **8**, 7643 (2018).
[7]W. Chen, F. So, and J. Guo, "Intrinsic delay of permeable base transistor," Journal of Applied Physics **116**, 044505 (2014).
[8]G. Gu and S. R. Forrest, "Design of flat-panel displays based on organic light-emitting devices," IEEE Journal of Selected Topics in Quantum Electronics **4**, 83–99 (1998).
[9]A. Al-Shadeedi, S. Liu, V. Kaphle, C.-M. Keum, and B. Lüssem, "Scaling of high-performance organic permeable base transistors," Advanced Electronic Materials **5**, 1800728 (2019).
[10]A. Al-shadeedi, S. Liu, R. K. Radha Krishnan, C.-M. Keum, V. Kaphle, D. B. Scott, and B. Lüssem, "Modeling tunnel currents in organic permeable-base transistors," Synthetic Metals **252**, 82 – 90 (2019).
[11]H. Sinno, S. Fabiano, X. Crispin, M. Berggren, and I. Engquist, "Bias stress effect in polyelectrolyte-gated organic field-effect transistors," Applied Physics Letters **102**, 113306 (2013).
[12]F. Colléaux, J. M. Ball, P. H. Wöbkenberg, P. J. Hotchkiss, S. R. Marder, and T. D. Anthopoulos, "Bias-stress effects in organic field-effect transistors based on self-assembled monolayer nanodielectrics," Phys. Chem. Chem. Phys. **13**, 14387–14393 (2011).
[13]R. A. Street, M. L. Chabinyc, F. Endicott, and B. Ong, "Extended time bias stress effects in polymer transistors," Journal of Applied Physics **100**, 114518 (2006).
[14]J. B. Chang and V. Subramanian, "Effect of active layer thickness on bias stress effect in pentacene thin-film transistors," Applied Physics Letters **88**, 233513 (2006).
[15]A. Salleo, F. Endicott, and R. A. Street, "Reversible and irreversible trapping at room temperature in poly(thiophene) thin-film transistors," Applied Physics Letters **86**, 263505 (2005).
[16]R. A. Street, A. Salleo, and M. L. Chabinyc, "Bipolaron mechanism for bias-stress effects in polymer transistors," Phys. Rev. B **68**, 085316 (2003).
[17]G. Paasch, "Transport and reactions in doped conjugated polymers: Electrochemical processes and organic devices," Journal of Electroanalytical Chemistry **600**, 131 – 141 (2007).
[18]B. Lüssem, M. L. Tietze, A. Fischer, P. Pahner, H. Kleemann, A. Günther, D. Kasemann, and K. Leo, "Beyond conventional organic transistors: novel approaches with improved performance and stability," Proceedings of SPIE **9185**, 91850H–1 (2014).
[19]K. Yutani, S. ya Fujimoto, K. ichi Nakayama, and M. Yokoyama, "Role of oxidation layer of aluminum base electrode in metal-base organic transistors," Molecular Crystals and Liquid Crystals **462**, 51–57 (2006).
[20]F. Kaschura, A. Fischer, M. P. Klinger, D. H. Doan, T. Koprucki, A. Glitzky, D. Kasemann, J. Widmer, and K. Leo, "Operation mechanism of high performance organic permeable base transistors with an insulated and perforated base electrode," Journal of Applied Physics **120**, 094501 (2016).
[21]S. Lee, B. Koo, J. Shin, E. Lee, H. Park, and H. Kim, "Effects of hydroxyl groups in polymeric dielectrics on organic transistor performance," Applied Physics Letters **88**, 162109 (2006).
[22]H. Klauk, U. Zschieschang, J. Pflaum, and M. Halik, "Ultralow-power organic complementary circuits," Nature **445**, 745 (2017).